



ORIGINAL ARTICLE

On the mechanical behavior of a hybrid reinforced concrete for industrial floors

Sobre o comportamento mecânico de um concreto com reforço híbrido para pisos industriais

Igor Nogueira Lima^a

Victor Nogueira Lima^b

Felipe Rodrigues de Souza^b

Felipe Pinheiro Teixeira^c

Maria Isabel Brasileiro Rodrigues^d

Flávio de Andrade Silva^b

^aPontifícia Universidade Católica do Rio de Janeiro – PUC-Rio, Department of Chemical and Materials Engineering, Rio de Janeiro, RJ, Brasil

^bPontifícia Universidade Católica do Rio de Janeiro – PUC-Rio, Department of Civil and Environmental Engineering, Rio de Janeiro, RJ, Brasil

^cUniversidade Estadual do Norte Fluminense Darcy Ribeiro – UENF, Postgraduate Program in Civil Engineering, Campos dos Goytacazes, RJ, Brasil

^dUniversidade Federal do Cariri – UFCA, Science and Technology Center, Juazeiro do Norte, CE, Brasil

Received 23 September 2022

Accepted 09 February 2023

Abstract: Civil construction is an industry sector that has been used as an outlet for the reuse of industrial waste. The present work aims to use the residue of Ethylene Vinyl Acetate (EVA) from the footwear industry as a partial substitute for a granulometric range of aggregates, aiming at the production of structural concrete and application to industrial floors. The proposed mixing ratios were evaluated from uniaxial compression, three-point bending, and drying shrinkage tests. The results of the uniaxial compression tests showed that the concrete with EVA addition still has enough strength to be considered structural concrete. In addition, the EVA and polypropylene fiber particles act as stress transfer bridges in the cracked zone, resulting in an increase in residual stresses and, consequently, in the toughness of the concrete in the three-point bending test. Finally, Technical Report 34 was used as a procedure to design an industrial floor based on the compressive strength, Young's modulus, and flexural behavior of the tested composites. The final result showed that even with lower compressive strength, fiber-reinforced concrete with EVA achieves greater structural efficiency for an industrial floor with the same cross-sectional height as ordinary fiber-reinforced concrete.

Keywords: EVA, concrete, fiber reinforced concrete, industry waste, toughness.

Resumo: A construção civil é um setor da indústria que tem sido utilizado como uma saída para o reaproveitamento de muitos resíduos. O presente trabalho visa utilizar o resíduo de Etileno Vinil Acetato (EVA) da indústria calçadista como substituto parcial de uma faixa granulométrica de agregados, visando produção de concreto estrutural e aplicação a concretagem de pisos industriais. As proporções de mistura propostas foram avaliadas a partir de ensaios de compressão uniaxial, flexão em três pontos e retração por secagem. Os resultados dos testes de compressão uniaxial mostraram que o concreto com substituição ainda apresenta resistência suficiente para ser considerado concreto estrutural. Além disso, as partículas de EVA e da fibra de polipropileno funcionam como pontes de transferência de tensões na zona fissurada, resultando em um aumento das tensões residuais e, conseqüentemente, da tenacidade do concreto no teste de flexão em três pontos. Por fim, o Technical Report 34 foi utilizado como procedimento para dimensionar um piso industrial a partir da resistência a compressão, módulo de Young e comportamento a flexão dos compósitos ensaiados. O resultado final mostrou que mesmo com menor resistência à compressão, o concreto reforçado com fibras e substituição parcial de EVA consegue maior eficiência estrutural para um piso industrial de mesma altura de seção transversal que o concreto reforçado com fibras comum.

Palavras-chave: EVA, concreto, concreto reforçado com fibra, resíduos da indústria, tenacidade.

How to cite: I. N. Lima, V. N. Lima, F. R. Souza, F. P. Teixeira, M. I. B. Rodrigues, and F. A. Silva, "On the mechanical behavior of a hybrid reinforced concrete for industrial floors," *Rev. IBRACON Estrut. Mater.*, vol. 16, no. 6, e16607, 2023, <https://doi.org/10.1590/S1983-41952023000600007>

Corresponding author: Victor Nogueira Lima. E-mail: eng.vnl@gmail.com

Financial support: This study was financed in part by the Coordenação de Aperfeiçoamento de Pessoal de Nível Superior (CAPES) – Brasil – Finance Code 001, by Brazilian funding agencies FAPERJ and CNPq, and by Lafarge Holcim, with the donation of cement.

Conflict of interest: Nothing to declare.

Data Availability: The data that support the findings of this study are available from the corresponding author, [VNL], upon reasonable request.



This is an Open Access article distributed under the terms of the Creative Commons Attribution License, which permits unrestricted use, distribution, and reproduction in any medium, provided the original work is properly cited.

1 INTRODUCTION

The industrialization process along with demographic and technological growth brought, in addition to the benefits, an increase in the generation of solid waste, causing environmental problems [1]–[3]. Because of this, many industry sectors are valuing the search for eco-friendly solutions to dispose of their waste. In the construction industry, for example, many researchers are concerned about how to reuse demolition waste as inert materials in the mixture of mortar and concrete [4]–[6].

In addition to the demolition waste, advances can be seen in the production of lightweight concrete using other types of waste as lightweight aggregate, which can lead to a decrease in compressive strength, a parameter that directly influences the quality of the cementitious material [7]–[11]. In this case, Ethylene Vinyl Acetate (EVA) is a residue that has been widely proposed for research focused on lightweight concrete formulations with permeable characteristics [12], [13] or for bituminous concretes [14], [15]. Most applications for this type of material are focused on paving [16], [17], and its use as an addition in structural concrete is a gap in the literature.

The use of plastic materials, such as the EVA mentioned above, has aroused much interest due to the difficulties encountered in disposing of the waste. As highlighted by Lima et al. [2], storage or disposal in landfills implies the availability of large surfaces, and incineration can emit potentially harmful gases and ashes. Because of this, the use of thermoplastic materials has become widespread in various sectors of the industry, as they can be melted in the recycling process [18]. However, EVA is not characterized as a thermoplastic material, but as a thermosetting material and, therefore, cannot be melted by heat due to its molecular chains.

In addition to EVA, some other plastic wastes have been destined for use as inert materials in concrete, i.e. polyethylene and polystyrene [19], [20], high-density polyethylene [21], polyethylene terephthalate (PET) [22], polyvinyl chloride (PVC) [23]. In general, the increase in the plastic content added to the mixture is inversely proportional to the density and strength of the cementitious material [24]–[27]. Li et al. [28] evaluated the variation of the apparent density and the incorporated air content of the cement paste and mortar samples with EVA additions. They noticed that when increasing the EVA content in the cement mixtures by up to 6%, there was a decrease in the apparent density and a significant increase in the content of incorporated air. Furthermore, Li et al. [28] pointed out a direct correlation between the EVA content and the compressive strength, showing that there is a reduction in the compressive strength with the increase of the amount of EVA in the mixture. Plastic aggregates reduce the strength of concrete when compared to ordinary concrete, mainly due to the low Young's modulus of plastic materials [26]. Therefore, the deformability of the material prevents the aggregate from functioning as a rigid core, not restricting displacement in its vicinity [27]. The impact of this substitution on Young's modulus is significant, ranging from 21 to 42% at levels of substitution up to 100% [27], [29].

On the other hand, some studies point out that the presence of plastic particulates can serve as bridges in cracks, mitigating the propagation of micro cracks and contributing to the toughness of the material [2], [30]. The EVA-modified concrete, using addition of EVA powder to the concrete mix, increases the flexural and tensile strength by incorporating up to 16% of EVA powder by weight of cement [31]. Thus, despite the impact on the strength of concrete, this material can have suitable applications, such as in situations where crack opening must be controlled or in cases where the structure is subject to impact loads [30].

Brovelli et al. [32] studied the influence of EVA on the rheology of bituminous concrete, comparing it with reference cases (without EVA addition). For all investigated samples, the addition of EVA increased the yield point and the plastic viscosity of the mixture. Furthermore, Ben Fraj et al. [33] performed slump tests comparing samples of ordinary concrete and concrete with partial replacement of aggregates by polyurethane. The results showed that the increase in rheological parameters observed by Brovelli et al. [32] was translated into a significant reduction in a slump test. They attributed this behavior to the fact that polymeric aggregates are quite porous, which facilitates the process of absorbing water from the mixture and cement paste, directly affecting workability. In addition to this mechanism, Alqahtani and Zafar [1] attribute the reduction in a slump to the increase in friction between the plastic particles, which leads to less fluidity. The large surface area of the particles coupled with the lack of uniformity in the geometry of the particles causes this friction [19], [34], [35].

Finally, aiming at the use of concrete with plastic aggregate for structures supported on an elastic base, i.e. industrial floors, it is important to understand the impact of replacement on the abrasion resistance and drying shrinkage of the material. In general, most studies highlight a significant increase in drying shrinkage for replacements of up to 80% [23], [36], [37]. This increase is attributed to the low rigidity and compressibility of the plastic material, which results in a low restriction to the shrinkage deformations induced by the cement paste [36], [37]. On the other hand, in the case of abrasion, Alqahtani et al. [24] showed that the abrasion resistance of concrete with indirect replacement of aggregates showed an increase of more than 50%. Alqahtani and Zafar [1] highlighted that the low strength and roughness of the plastic aggregate, when compared to the common aggregate, was the main responsible for this increase in abrasion resistance.

Moreover, discrete synthetic fiber addition, such as polypropylene (PP), has been used primarily to reduce shrinkage effects [38]. Fibers also mitigate crack propagation and improve impact resistance, flexural and tensile strengths [39]–[41], toughness [41], [42], and abrasion resistance [43]. For use in concrete pavements, where high flexural strength is required, PP fibers contribute to reducing the concrete design thickness, and the pavement integrity remains even after the crack formation [44]–[46].

Hybrid EVA particle and PP fiber-reinforced concretes have been also addressed in the literature [47], [48]. The flexural performance of PP-EVA hybrid reinforced concrete is improved as the maximum and residual flexural strength increase up to 11% when compared to ordinary concrete, and up to 4% when compared to polypropylene fiber reinforced concrete (PP-FRC) [47]. Besides, an improvement of around 40% in the toughness can be seen in the PP-EVA hybrid reinforced concretes compared to a PP-FRC with the same fiber content [47].

Although several studies have already addressed the basic properties of concrete with the replacement of aggregates by recycled plastic aggregates and also the fiber inclusion, few works have sought to replace an existing granulometric range, and none clearly addressed the use in industrial floors, adding a fiber content consistent with the proposed field application. Knowing that the replacement directly affects the strength and elastic properties of the cementitious material, this work proposes the use of polypropylene plastic fibers as a way to improve the control of crack propagation, directly impacting the ability to absorb energy. In addition, a comparison between an industrial floor calculated using the properties of ordinary concrete is compared to the proposed material.

2 MATERIAL AND METHODS

2.1 Materials

The cement used was a Portland cement CP V ARI from the manufacturer Lafarge Holcim, which is equivalent to ASTM type III according to Natalli et al. [49]. This cement type, according to the Brazilian standard NBR 16697/18 [50], has a minimum compressive strength of 34 MPa at 7 days when mixed in a standard 1:3 mortar, and the results for the used cement batch are presented in Table 1. In addition to the mechanical characteristics, chemical tests were carried out on this batch of cement, and the results are shown in Table 2.

Table 1. Compressive tests for the batch of cement used in the research.

Tests	Mean [SD]*	Requirement**
Compressive strength 1 day (MPa)	24.5 [1.45]	≥ 14
Compressive strength 3 days (MPa)	34.4 [1.35]	≥ 24
Compressive strength 7 days (MPa)	40.5 [1.05]	≥ 34
Compressive strength 28 days (MPa)	48.8 [1.11]	not applicable

*Standard deviation. **According to NBR 16697/18

Table 2. Chemical tests for the cement batch used in the research.

Tests	Standards	Unit	Mean	Requirement*
SO ₃	NM 16/12	%	3.17	≤ 4.5
IR	NM 22/04	%	1.58	≤ 1
CaO _{free}	NM 13/13	%	1.97	not applicable
MgO	NM 14/14	%	1.71	≤ 6.5

SO₃ - determination of the sulfur trioxide content in the composition. IR - the percentage of insoluble residue in the composition. CaO_{free} - determination of the free calcium oxide content in the composition. MgO - determination of the magnesium oxide content in the composition. *According to NBR 16697/18

Two coarse granite aggregates were included in the mix design: one with a maximum diameter of 9 mm and the other with 19 mm. In addition, natural quartz sand and mineral stone sand were used as fine aggregates. Natural quartz sand has a maximum characteristic dimension of 4.75 mm and a fineness modulus of 2.74, and mineral stone sand has a maximum dimension of 2.40 mm and a fineness modulus of 2.02. Therefore, both are classified as fine aggregates in the optimal zone according to NBR 7211 [51]. In addition, EVA was also used as a mixing material. The EVA used is a waste from the footwear industry in the countryside of the state of Ceará in Brazil, and it is found in a carved condition with a granulometry close to the 9 mm diameter coarse aggregate mentioned above. The granulometry of the aggregates and EVA are shown in Figure 1.

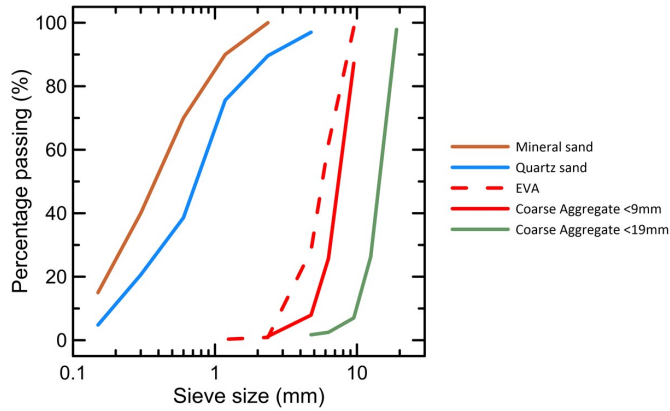


Figure 1. Aggregates granulometric distribution curve.

Although the EVA particles present a granulometric curve similar to the 9 mm coarse aggregate, their shape is quite irregular and predominantly two-dimensional, as seen in Figure 2. Therefore, evaluation of the shape of the particles with the aid of a Nikon microscope model SMZ800N and through image processing using the Image J software was done. Figure 2 shows the segmentation performed and the binary images generated for the total area of the particles analyzed, with a resolution of 1596x1064 pixels. Then, data related to the analysis of particles was obtained through the segmented image. The data obtained are summarized in Table 3.

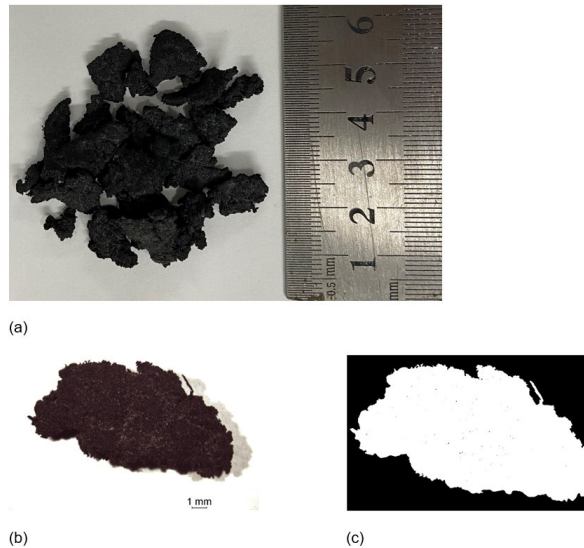


Figure 2. EVA carved particles and microscopic analysis of one EVA particle. (a) EVA carved samples, (b) image of the EVA particle obtained through a Nikon microscope model SMZ800N, and (c) binary image resulting from the segmentation.

Table 3. Summary of geometric measurements of EVA particles accessed by microscopy technique.

Particle	Total Area (mm ²)	Perimeter (mm)	Circularity
EVA 1	75.54	15.81	0.77
EVA 2	84.33	54.29	0.36
EVA 3	81.54	53.06	0.36
EVA 4	80.08	47.75	0.44
EVA 5	68.51	25.91	0.66
Mean	78.00	39.36	0.52
Standard Deviation (SD)	6.18	17.44	0.19

The results obtained from five EVA particle samples show that the EVA particles have a total area of $78 \pm 6.18 \text{ mm}^2$, which means $46.01 \pm 3.61\%$ of the total area considering the image background. Due to the irregularity of the particles, it can be noted that the perimeter varies considerably concerning the calculated average, with values of $39.36 \pm 17.44 \text{ mm}$, different from the low standard deviation found for the particle area values. This consideration becomes even clearer when the circularity of the particles is evaluated, which resulted in 0.52. The circularity parameter is a dimensionless measure obtained through a metric used in image processing and analysis techniques, defined by $C=4\pi \times (A/P^2)$, where A is the area of the particle and P is the perimeter of the particle. The reference value of the circularity parameter is 1, representing the perfect circle. Therefore, as the value approaches 0, an increasingly elongated shape is indicated. Furthermore, an X-ray Fluorescence analysis (XRF) was performed on the EVA, and the elements and their respective amounts found are presented in Table 4.

Table 4. Composition of the EVA generated by the XRF analysis.

Composition	Content	Unit
Si	3060	ppm
Si	71.2	ppm
Cl	779.9	ppm
Ca	2.58×10^5	ppm
Ti	2.85×10^4	ppm
V	105.1	ppm
Mn	44.0	ppm
Fe	573.2	ppm
Cu	251.1	ppm
Zn	4×10^4	ppm
Sr	81.1	ppm
Zr	55.1	ppm
Sm	54.5	ppm

The polypropylene (PP) fibers used in this work were the 51 mm length Viapol TUF-Strand SF[®] with an aspect ratio of 74. The main characteristics and properties of these macro fibers are presented in Table 5. The fibers have twisted geometry, which aims to facilitate the mixing procedure, as well as improve the mechanical anchorage at the fiber-matrix interface. In addition, each fiber is the result of the union of about 3 strands grouped, giving the fiber irregular cross-sections along its length, as seen in Figure 3.

Table 5. Polypropylene fiber properties provided by the manufacturer.

Density (g/cm ³)	0.92
Length (mm)	0.51
Aspect ratio (l/d)	74
Tensile strength (MPa)	625
Modulus of elasticity (Gpa)	9.5
Fusion point (°C)	160
Thermal and electrical conductivity	Low
Water absorption	Negligible
Resistance to alkali and acids	Excellent

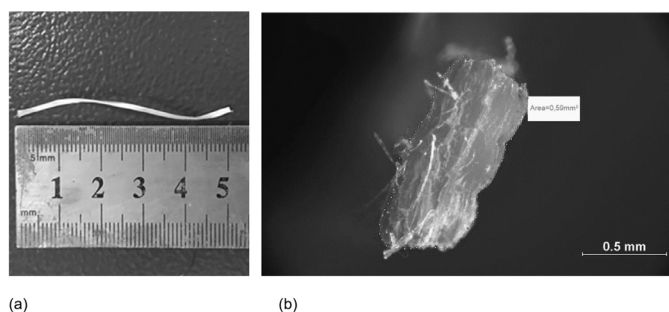


Figure 3. Polypropylene fiber with 51 mm length. (a) Image presenting the PP twisted geometry and (b) Image of the PP fiber cross section obtained through a Nikon microscope model SMZ800N.

2.2 Mixing design

The dosage of the structural concrete matrix used is shown in Table 6, considering the mixture proportion of ordinary concrete (OC), concrete with the volume replacement of coarse aggregate by EVA (EVA-C), PP fiber reinforced concrete (FRC), and the concrete with replacement of coarse aggregate by EVA reinforced with PP fiber (EVA-FRC). The mixing procedure was started by adding the aggregates (quartz sand, mineral sand, coarse aggregates, and EVA) which were mixed with 70% water for one minute. Then, cement was added to the mixture and allowed to mix for another minute. The remaining water was added to the mixture with the superplasticizer chemical admixtures, which was used to give better workability to the concrete. The superplasticizer admixture used was PLASTOL® 4100, produced by the manufacturer VIAPOL, characterized as type SP-II N by the NBR 11768 standard [52]. The superplasticizer content was adjusted from the slump test following NBR NM 67 [53] before starting the specimens molding process. For the mixtures containing polypropylene (PP) fibers, a final step was added to the procedure to throw and let the fiber disperse, following the time target stated by Lima et al. [41].

Table 6. Mixture compositions of the concretes used, considering the ordinary concrete (OC), the concrete with replacement of coarse aggregate by EVA (EVA-C), PP fiber reinforced concrete (FRC), and the concrete with replacement of coarse aggregate by EVA reinforced with PP fiber.

Material type	OC	EVA-C	FRC	EVA-FRC
	kg/m ³			
Cement (CPV ARI)	380	380	380	380
Quartz sand	675	675	675	675
Mineral sand	136	136	136	136
Coarse aggregate (maximum diameter 9 mm)	250	-	250	-
EVA	-	51	-	51
Coarse aggregate (maximum diameter 19 mm)	650	650	650	650
Water	190	190	190	190
Superplasticizer	1.52	1.52	1.52	1.52
Polypropylene fiber	0	0	5	5

All samples were cured in a room with controlled temperature and humidity (23°C and 100%) for 28 days before mechanical testing. On the twenty-eighth day, the specimens were removed from the curing room and taken to the specimen preparation room. Finally, on the twenty-ninth day, the mechanical tests commenced.

2.3 Density measurements

The variation of concrete density was measured by weighing cylindrical specimens measuring 10 x 20 cm. For this test, the samples destined for the compressive strength test were weighed before the destructive test. Knowing the weight and volume of the sample, the approximate apparent density of the materials was calculated. It can be seen in Table 7 that the density variation was not so significant, and this is since only the coarse aggregate with a 9 mm maximum particle size was completely replaced by the EVA aggregate. Thus, the coarse aggregate with a maximum particle size of 19 mm and the natural and mineral sands remained as constituent materials of the mixture. Therefore, in terms of weight, there is a 10% weight relief of concrete with EVA (EVA-C) compared to ordinary concrete (OC).

Table 7. Approximate apparent density for the two analyzed concretes (OC and EVA-C).

Specimen	Volume (m ³)	Weight (Kg)	Density (Kg/m ³)
EVA-C	0.0015	3.374 ± 0.152	2249 ± 114
OC	0.0015	3.682 ± 0.197	2455 ± 125

2.4 Mechanical tests

The experimental mechanical characterization and testing of concretes evaluated include measurement of uniaxial compressive strength and a 3-point bending test controlled by the crack mouth opening displacement. From the mechanical results obtained, it is possible to verify the application of the material developed for industrial floors, drawing a comparison between the OC and the EVA-C.

2.4.1 Uniaxial compressive strength

Uniaxial compressive strength test and Young’s modulus estimation were done at 28 days, according to NBR 5739 [54] and NBR 8522 [55] standards. Cylinders of 100 mm in diameter and 200 mm in height were cast. Before this process, the molds were prepared with a release oil coat for then the concrete to be poured. Its densification was done by external vibration, initially with a rubber hammer and then on a vibrating table. After 24 hours, the specimens were demolded and taken to an environment of controlled temperature and humidity (humid chamber). Approximately 24 hours before the test, the specimens went through the process of gridding the base and the top to ensure the regularity of the surface and parallelism between the faces. It ensures that the transfer of stresses during loading is uniform.

The tests were carried out in a servo-controlled Controls testing machine model MCC8, with a load capacity of 2000 kN and a loading speed of 0.35 MPa/s. For higher precision of Young’s modulus, two vertical displacement transducers (LVDT) attached to cylindrical rings were fixed around the specimen to measure the deformation, as can be seen in the scheme of Figure 4. In this way, the value of the specimen’s deformation was obtained by the relation between the average value of the measured relative displacement and the initial length of reference given by the distance between the rings. Stress was calculated as the ratio between the applied load and the cross-sectional area of the specimen. Young’s modulus corresponds to the slope of the initial region of the stress versus strain curve, up to approximately 30% of the maximum stress.

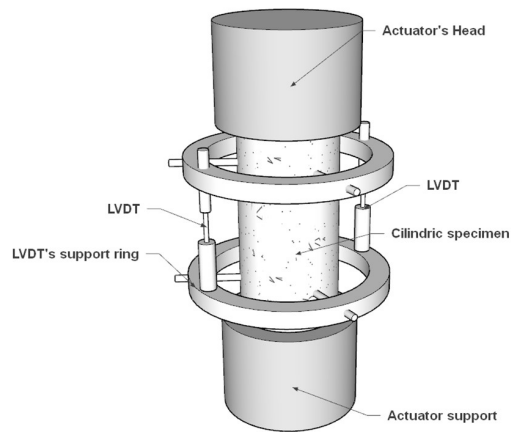


Figure 4. Uniaxial compressive strength setup detailing the cylindrical rings and LVDTs positions.

2.4.2 Three-point bending test

Three-point bending tests were performed on prismatic elements of rectangular sections, following the standard EN 14651 [56]. The dimensions of the specimens were 150 x 150 x 550 mm, with a 25 mm high notch in the central region of the lateral face of the prisms made with a 3 mm thick diamond saw. For molding the concrete samples, the mixture was carried out in a concrete mixer with a capacity of 400 l, following the procedure described in section 2.2.

To assemble the test apparatus, support rollers were first positioned. The rollers were 37 mm in diameter, with a 500 mm span, and 25 mm from the edges of the prisms. The rollers had freedom of horizontal movement, however, the left roller had also freedom of transverse movement. This freedom for horizontal displacements prevents the induction of horizontal reactions in the supports and, consequently, the appearance of an eccentric normal force in the structural element, which would cause a change in the stress distribution.

The load application roller was free to move in the transverse direction and had the same diameter as the support rollers. The load application was centered on the top face of the prism. The test equipment used was an MTS model 244.41 servo-hydraulic actuator with a 500 kN loading capacity. To control the piston displacement, a clip gauge and a flex-test 60 controller were used, resulting in a closed-loop system.

The Crack Mouth Opening Displacement (CMOD) values were obtained using an MTS clip gauge model 632.02B-20, fitted to metallic plates fixed to the specimen in the region of the notch Figure 5. The CMOD was adopted as control parameter of the test, carried out at a displacement rate of 0.05 mm/min, to a crack width of 0.1 mm, and then at a rate

of 0.2 mm/min to a crack width of 4 mm. Data were acquired at a frequency of 5 Hz. The geometry of the prismatic specimen and the test setup is shown in Figure 5.

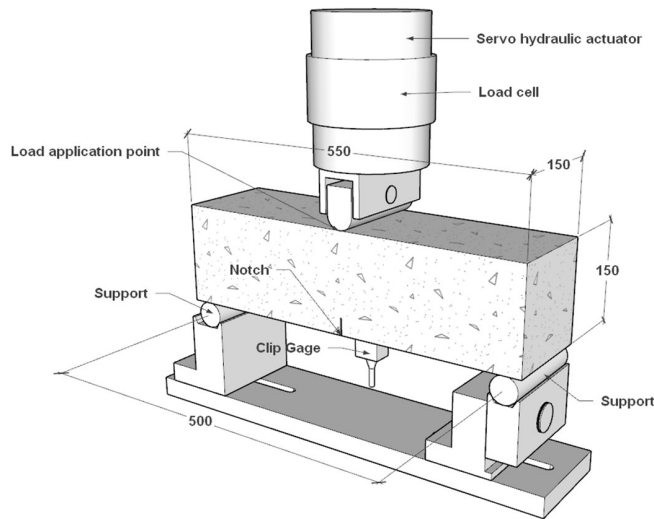


Figure 5. Flexural specimens' geometry, setup of the three-point bending test, and positioning of the clip gauge to measure the crack mouth opening displacement (CMOD).

From the test results, it is possible to plot the stress versus CMOD curves, considering the stress values obtained from Equation 1. The term P refers to the load, S to the test span, b to the width of the specimen, and h_{sp} is the distance between the top of the notch and the top face of the prism.

$$\sigma = \frac{3PS}{2bh_{sp}^2} \quad (1)$$

The advantage of this kind of test is that, due to the presence of the notch in the central region of the specimen, the crack formation is induced to occur in an orientated way, propagating itself along cross-section. In this way, the deformation is always localized, which minimizes energy dissipation throughout the test specimen. Therefore, all the energy absorbed can be directly associated with the fracture along the notch plane and all the energy dissipated can be correlated with the response of the evaluated concrete.

Furthermore, the fib Model Code [57] recommends the determination of residual stresses $f_{R,1}$ and $f_{R,3}$. The stress $f_{R,1}$ corresponds to a crack width of 0.5 mm and is related to the serviceability limit state. On the other hand, the stress $f_{R,3}$ corresponds to a crack width of 2.5 mm and is related to the ultimate limit state. It should also be noted that, according to EN 14651 [56], two other residual stresses refer to the crack openings of 1.5 and 3.5 mm, respectively called $f_{R,2}$ and $f_{R,4}$. The last important parameter that must be obtained through the three-point bending tests is the toughness at the 4 mm crack opening ($T_{4,0}$), calculated as the area under force per CMOD curve. This parameter indicates the material's ability to absorb energy.

2.4 Drying shrinkage test

Drying shrinkage tests were performed according to ASTM C157 [58] and ASTM C490 [59] standards, in order to estimate the magnitude of the stress independent strain in the two types of concrete studied (Figure 6). Three prisms measuring 75 x 75 x 285 mm were molded for each of the mixtures. The molding was performed in the same test room, with controlled temperature and relative humidity ($20 \pm 1^\circ\text{C}$ and $50 \pm 5\%$). Strain readings were taken once a day from the first measurement to 28 days of age. From then on, measurements were taken weekly.

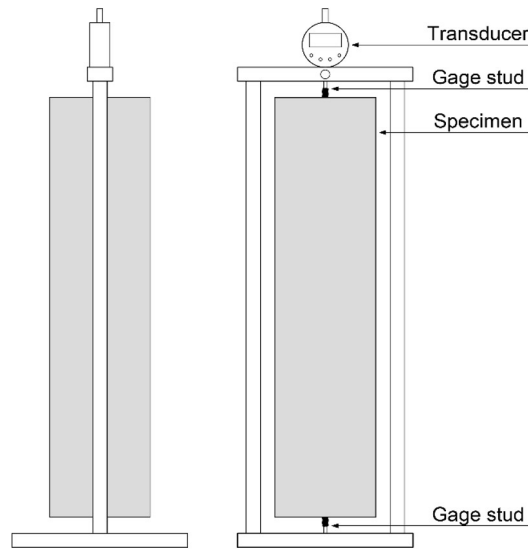


Figure 6. Drying shrinkage test setup.

2.4 Considerations for numerical approach

Since the main application of fiber-reinforced concrete is aimed at ground-supported industrial floors, we decided to make a comparison between an industrial floor designed for the conventional FRC concrete and another designed for the EVA-FRC. For this analysis, Technical Report 34 [60] was used, and only the case of internal loading was considered, not taking into account the case of loading at the borders of the floor (Figure 7).

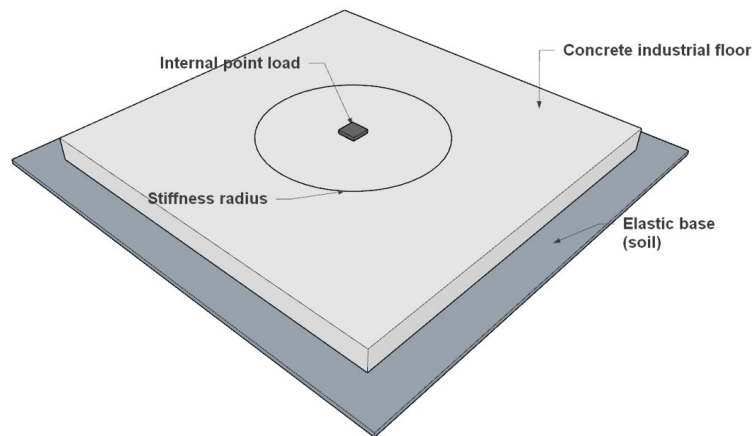


Figure 7. Schematic drawing of the type of loading used to calculate the industrial floor (internal loading) according to [60].

3 RESULTS AND DISCUSSIONS

3.1 Uniaxial compressive strength

According to the test procedure described in Section 3, uniaxial compressive strength tests were performed for ordinary concrete (OC) and concrete with total replacement of the coarse aggregate of smaller diameter by EVA (EVA-C). In addition, the inclusion of fibers was considered in this test stage, evaluating the behavior of the two concretes with the inclusion of 5 kg/m^3 of polypropylene fiber (FRC and EVA-FRC). The results of compressive strength and Young's modulus are shown in Figure 8. It is noteworthy that the results obtained correspond to the average of the results of 5 tests for each specimen group.

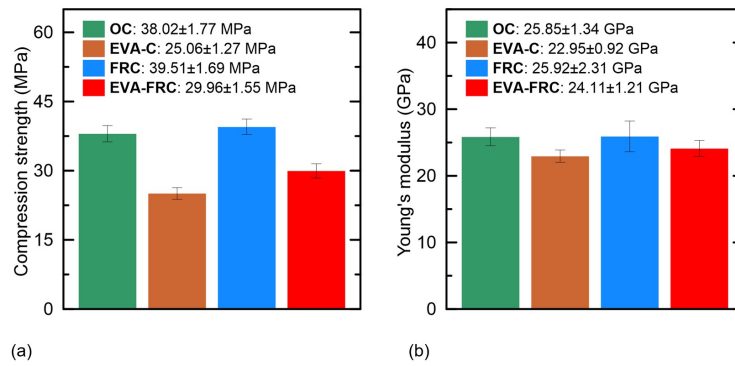


Figure 8. Uniaxial compressive strength results for the four types of concrete evaluated. (a) Maximum compressive strength and (b) Young's modulus.

In the cases of concrete with aggregate replacement by EVA (EVA-C and EVA-FRC), a drop in compressive strength was noticed when compared to the results of ordinary concrete (OC and FRC). This difference may have been caused by the reduction in the compacity of the aggregates, generating critical areas with stress concentrations in the vicinity of the EVA particles that are significantly more deformable than the conventional aggregate [2], [61]. It is known that rock aggregates help in the compaction of the material, improving cohesion and friction angle, and in cases where there are shear stresses, the aggregate helps in interlocking [62], [63]. In the case of EVA, meshing and interlocking are impaired, but an improvement in material toughness can be expected, a property that will be evaluated with bending tests.

Yang et al. [64] performed compressive strength tests on cement modified with EVA for underground gas storage, varying the percentage of EVA particle inclusion by volume (1%, 2%, 3%, and 4% EVA). The results showed that there is a decrease in the compressive strength of the samples from 3% for the addition of 1% EVA to 14% for the addition of 4% EVA. Li et al. [65] and Lima et al. [2] addressed in their studies a greater inclusion of EVA by volume, considering 10% addition and 50% replacement of aggregate respectively. Consequently, this level of inclusion of EVA in the mixture resulted in a more significant reduction in the compressive strength of the samples, reaching values about 40% and 70% lower than the reference case. In the present work, as the total replacement of only one granulometric range was carried out, the reduction of the compressive strength did not reach the same magnitude found by Lima et al. [2] for the replacement of 50% of the aggregates. Comparing OC and EVA-C the reduction of compressive strength was 33% and comparing FRC and EVA-FRC this reduction was less significant reaching 20%.

As for the fiber-reinforced concrete (FRC) specimen, the compressive strength result was higher than the conventional concrete (OC) strength, and this may have happened due to the contribution of the fibers acting as a confinement agent for the concrete, resulting in a better distribution of the applied stresses [66]. However, it is known that the fibers have little influence on the compressive and tensile strength of concrete, being quite effective in the post-peak [67]. Therefore, it is likely that this difference of 1 MPa is more correlated to the variability of the results since concrete is a heterogeneous material than to an improvement in strength.

Finally, when comparing only the EVA-FRC and EVA-C concretes, it can be seen that the fibers may be contributing to the improvement of uniaxial compressive strength. It is known that concrete with aggregates with lower Young's modulus, such as EVA, can lose the ability to mesh and interlock, starting to concentrate stress in the vicinity of the EVA [68]. Thus, the inclusion of fibers in the mixture can improve the interlocking capacity of the material, serving as a bridge for the stress transfer to the microcracks that may arise.

3.2 Three-point bending test

The efficiency of fibers as reinforcement depends mainly on interactions at the interface and includes chemical, frictional adhesion, and mechanical anchoring. Chemical adhesion corresponds to the primary adhesion of the interface, which is the result of chemical reactions from the composition of both the fibers and the matrix [38]. To evaluate the efficiency of the reinforcements with polypropylene fiber and the addition of EVA, bending tests were performed with monotonic loading as established in Section 3.

Table 8 and Table 9 present the results of the three-point bending test. For each type of concrete evaluated, three tests were carried out, with the values expressed as the final result corresponding to the average of the results obtained, followed by its standard deviation.

Table 8. Summary of three-point bending test parameters.

Specimen	P_{LOP} (KN)	σ_{LOP} (MPa)	$CMOD_{LOP}$	$f_{R,1}$ (MPa)	$f_{R,2}$ (MPa)	$f_{R,3}$ (MPa)	$f_{R,4}$ (MPa)
OC	13.07 [1.14]	4.18 [0.11]	0.034 [0.017]	-	-	-	-
EVA-C	12.65 [0.80]	4.05 [0.26]	0.049 [0.001]	1.04 [0.09]	0.34 [0.05]	0.19 [0.03]	0.12 [0.02]
FRC	14.66 [1.09]	4.22 [0.31]	0.046 [0.003]	1.47 [0.07]	1.49 [0.09]	1.49 [0.09]	1.38 [0.09]
EVA-FRC	13.88 [0.94]	4.00 [0.27]	0.044 [0.006]	1.97 [0.16]	1.94 [0.16]	1.99 [0.29]	1.98 [0.30]

P_{LOP} = load corresponding to the limit of proportionality; σ_{LOP} = stress corresponding to the limit of proportionality; $CMOD_{LOP}$ = crack opening corresponding to the limit of proportionality; $f_{R,1}$ = residual flexural strength corresponding to 0.5 mm CMOD; $f_{R,2}$ = residual flexural strength corresponding to 1.5 mm CMOD; $f_{R,3}$ = residual flexural strength corresponding to 2.5 mm CMOD; $f_{R,4}$ = residual flexural strength corresponding to 3.5 mm CMOD;

Table 9. Peak stress maintenance and toughness results.

Sample	$f_{R,1}/\sigma_{LOP}$	$f_{R,2}/\sigma_{LOP}$	$f_{R,3}/\sigma_{LOP}$	$f_{R,4}/\sigma_{LOP}$	$f_{R,3}/f_{R,1}$	$T_{4,0}$ (J)
EVA-C	0.25 [0.02]	0.08 [0.01]	0.05 [0.01]	0.03 [0.01]	0.18 [0.02]	6.63 [0.56]
FRC	0.35 [0.04]	0.35 [0.04]	0.35 [0.04]	0.33 [0.04]	1.01 [0.01]	21.5 [1.18]
EVA-FRC	0.52 [0.08]	0.53 [0.08]	0.55 [0.07]	0.55 [0.06]	1.05 [0.02]	30.24 [1.04]

$f_{R,i}/\sigma_{LOP}$ = peak stress maintenance; $T_{4,0}$ = toughness up to 4.0 mm CMOD.

As recommended by standard EN 14651 [56], the characteristic parameters of concrete were obtained from the tests carried out. Among them, proportionality limit (σ_{LOP}), that is defined as the stress corresponding to the maximum load within the crack width range from 0 to 0.05 mm. The value of the ultimate load (P_U) was also determined, being the point where the slope of the load versus the CMOD curve is null. In addition, residual stresses were obtained at pre-defined CMOD values, 0.5, 1.5, 2.5, and 3.5 mm, and toughness values were defined as the area under the load versus CMOD curves. For the toughness, the limit point considered for the calculation was the end of the test, that is, a crack opening of 4 mm.

Figure 9 and Figure 10 show the stress per CMOD and toughness per CMOD curves, respectively, of all composites evaluated. It is observed that all curves displayed a linear behavior until the appearance of the first crack, followed by a decrease in stress with increasing CMOD. This behavior is called deflection softening and is characterized by the appearance of a single crack, common in composites reinforced with discrete fibers [69]–[71]. Therefore, in all cases, the ultimate load value corresponds to the load at the proportionality limit (P_{LOP}).

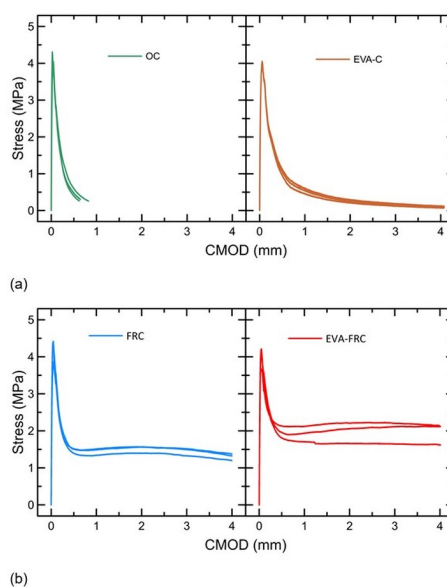


Figure 9. Stress versus CMOD graphs of the 3-point bending test for the four concretes evaluated (OC, EVA-C, FRC, and EVA-FRC). (a) Ordinary concrete and EVA concrete and (b) Fiber reinforced concretes considering the OC based and EVA based concretes as matrices.

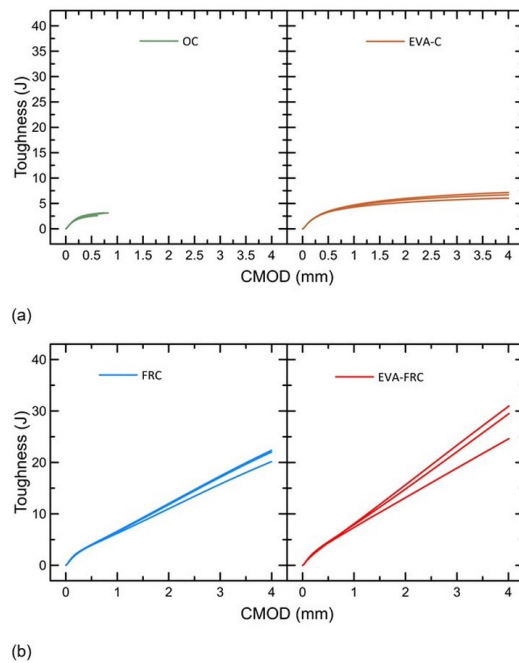


Figure 10. Toughness versus CMOD graphs of the 3-point bending test for the four concretes evaluated (OC, EVA-C, FRC, and EVA-FRC). (a) Ordinary concrete and EVA concrete and (b) Fiber reinforced concretes considering the OC based and EVA based concretes as matrices.

For all composites, the appearance of the first crack is related to the strength of the matrix and, therefore, it can be verified for OC the typical behavior of brittle material with immediate loss of strength after cracking. For FRC, after cracking, the fibers begin to absorb the tensile stresses in the cracked region, making the material behave in a pseudo-ductile manner. In the case of the three-point bending test, and considering the combinations investigated, the ultimate strength presented an average variation of 5.32% when comparing the fiber-reinforced plain concrete (FRC) and the EVA fiber-reinforced concrete (EVA-FRC).

Although the pre-cracking behavior was similar, the post-cracking behavior varied. The use of fibers improves the mechanical behavior of concrete, especially toughness and post-cracking residual strength. Table 9 presents the relationship between the residual stresses and the ultimate composite stress ($f_{R,i}/\sigma_{LOP}$), defined as relative residual strength. It is considered that the greater the value of this ratio, the greater the ability of the composite to maintain its strength after the appearance of the first crack. The evaluation of these values allows us to characterize the efficiency of the reinforcement in absorbing the stresses to which they are submitted. In the case of EVA-C, the strength capacity at serviceability state was maintained at approximately 25%. For the case of the FRC, the strength capacity observed was 35% while in the EVA-FRC it resulted in an average strength capacity of 52%. These results indicate that the addition of EVA hybridized with the addition of fibers improves the maintenance of the post-peak strength capacity for the concrete evaluated.

Another way of evaluating the influence of fibers on concrete is through the toughness, which reflects the energy absorption capacity of the material. Thus, it can be seen that both composites resulted in toughness greater than 20 J. The EVA-FRC reached a toughness resultant of about 30 J, which shows that not only the fiber but also the EVA is somehow bridging the crack opened.

4 NUMERICAL APPROACH

4.1 Fib Model Code simplified model

Using the simplified model of the fib Model Code (Figure 11) and considering that the ultimate tensile strength is defined by the residual stress $f_{R,3}$, assuming that the compressive stress resultant is applied on the extrados chord and that the tensile behavior is rigid-linear, it is possible to estimate the moment associated with this ultimate stress and calculate the contribution of EVA in terms of the resistant moment of the section. Thus, calculating the moment equivalent to the CMOD 2.5 mm (CMOD₃), the FRC resulted in a resistant moment of 53.90 kN.cm and the EVA-FRC

resulted in a resistant moment of 77.34 kN.cm. Therefore, EVA-FRC has a moment resistance of approximately 43.5% higher than conventional FRC, presenting by constitutive law that the EVA plays a role in bridging the fractured section.

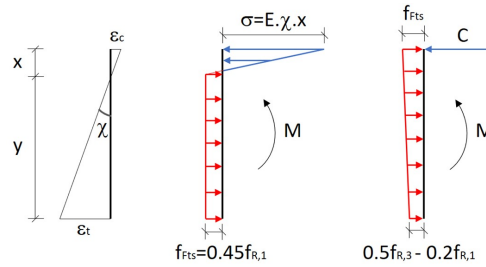


Figure 11. Fib Model Code simplified model to compute the ultimate tensile strength in uniaxial tension f_{FTu} by means of the residual nominal bending strength $f_{R,3}$ [57].

4.2 Industrial floor design based on Technical Report 34

It should be noted that the constitutive law of the material for this application differs from that described by the fib Model Code since, in this case, the structural element is supported on an elastic media (soil). In this way, Figure 12 presents the constitutive law of the material that now depends on $f_{R,1}$ and $f_{R,4}$ and no longer on $f_{R,3}$. Hence, the conservatively calculated ultimate moment can be estimated according to Equation 2.

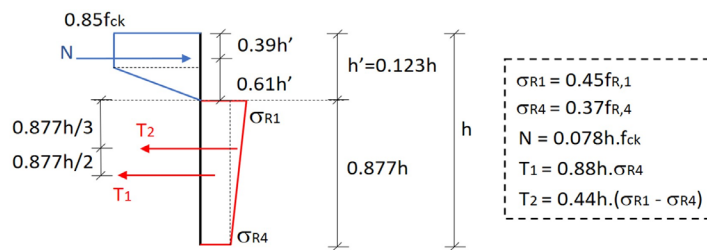


Figure 12. Fiber reinforced concrete constitutive law for ground supported floors according to Technical Report 34 [60].

$$M_u = \frac{h^2}{\gamma_m} (0.29\sigma_{r4} + 0.16\sigma_{r1}) \tag{2}$$

From the data obtained through the compressive test (compressive strength and Young’s modulus) and the three-point bending test (matrix flexural strength, residual stresses, and toughness), the necessary dimension for an industrial floor was calculated using the two FRCs and considering an elastic base of 0.048 N/mm³. As well, it should be noted that the partial safety factor for materials was applied for the ultimate limit state case ($\gamma_{m,uls}=1.5$). An isolated point load of 5 tf/pallet end support and 6 tf/axle for forklift traffic were adopted for calculation. The summary of the dimensions and degree of use (M_{calc}/M_{adm}) considering the loads adopted are shown in Table 10. The design results showed that even with lower compressive strength and a not so significant decrease in the tensile strength of the matrix in bending, the EVA-FRC achieves greater structural efficiency for an industrial floor of the same cross-sectional height (13 cm).

Table 10. Summary table of the efficiency of FRC and EVA-FRC applied in the design of industrial floors.

Material	Cross section height (cm)	Mcalc/Madm (pallet support)	Mcalc/Madm (forklift)
FRC	13	97%	90%
EVA-FRC	13	91%	84%

Therefore, the carved EVA is functioning as a support to the fibers in the crack bridge. This hypothesis makes sense, as the aggregates that intercept a crack tend to rupture or be completely pulled out at the moment of the matrix rupture.

In the case of carved EVA, as it is a flexible material, it may be stretched and pulled out after the appearance of the crack in the cement matrix, and thus the bending behavior of the concrete with EVA has a certain ductility, further improving the pseudo ductile behavior of fiber-reinforced concrete.

Industrial floors are subject to the stress of loads and potentially from restraint to drying shrinkage, and this combination can cause cracking [44], [45], [72]. A realistic evaluation of the combined effects of stresses induced by load and shrinkage is problematic and can produce conservative designs without significantly reducing the risk of cracking. Hence, Technical Report 34 [60] recommends an approach that does not take into account the effect of stresses induced by shrinkage, minimizing shrinkage by focusing on the design of the concrete mix, and constraining shrinkage with careful attention to the design and construction of the sub-base. In addition, Technical Report 34 [60] sets average drying shrinkage of the order of 300 $\mu\text{m/m}$ – 450 $\mu\text{m/m}$. Thus, although the concrete with aggregate replacement by EVA residue presents a significant efficiency for the application on industrial floors, it must be ensured that the concrete drying shrinkage does not exceed recommendations limits.

From a drying shrinkage point of view, the main effect of the aggregate is to restrict the contraction of the cement paste, thus helping to reduce the likelihood of cracking. In general, aggregates with a higher Young’s modulus, cubic shape, and rough particle surface textures tend to offer more restraint to concrete shrinkage [73]–[76]. However, the EVA used in this work has a low modulus of elasticity and an approximately two-dimensional shape, which can result in a significant increase in drying shrinkage even considering only partial replacement of the aggregates.

Therefore, drying shrinkage tests were performed according to ASTM C157 [58] and ASTM C490 [59] standards. Figure 13 shows the results of the drying shrinkage test for ordinary concrete and concrete with aggregate replacement by EVA, considering three specimens for each group tested. It can be seen from the analysis of the curves that the granular skeleton of the concrete with replacement still considerably restricts the shrinkage and, therefore, even with the presence of EVA in the composition, which is a flexible and easily deformable material, the coarse aggregate 19 mm in diameter and the fine aggregates can contain the deformation of the bulk cement paste.

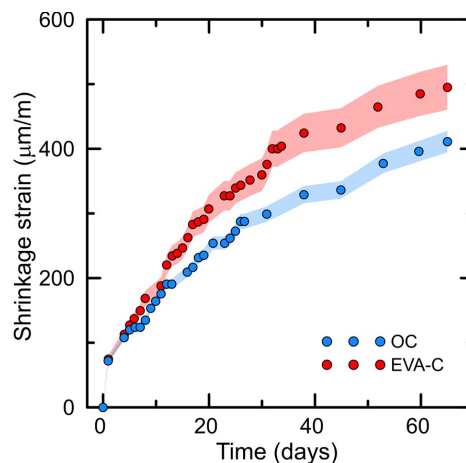


Figure 13. Schematic drawing of the type of loading used to calculate the industrial floor (internal loading) according to Technical Report 34 [60].

However, considering the shrinkage limit imposed by Technical Report 34 [60], the average shrinkage of EVA-C around 500 $\mu\text{m/m}$ exceeds this limit. Therefore, aiming at the application of this material for industrial floors, chemical expander admixtures must be used in addition to the already widespread wet curing and/or chemical curing processes.

5 CURRENT STUDY LIMITATIONS AND UNCERTAINTY

From a material point of view, the residue substitution limits need to be addressed, carrying out tests with various residue contents and verifying the design of the mixture. In addition, one should seek to understand the effect of EVA replacement on the rheological properties of concrete and the possible impacts on durability, from a chemical to a mechanical point of view with creep and fatigue tests. In the case of the composite, the work presented only one type of reinforcing fiber and only one fiber volumetric fraction. These points need to be variables for future studies to

characterize the contribution of EVA particles to different fibers and different fiber contents. Finally, experimental analysis on a structural scale needs to be carried out to validate the use of this material and verify if the industrial floor design proposed in this work is valid in practice.

6 CONCLUSIONS

This paper presents valuable information on the influence of EVA particles on the mechanical properties of plain and fiber-reinforced concrete. Density, drying shrinkage, uniaxial compressive strength, and three-point bending tests were performed to draw the following conclusions:

- EVA particles have dimensions and granulometric distribution of approximately 9 mm coarse aggregates with 23% lower density.
- With the total replacement of the 9 mm stone aggregate by the EVA particles residue, lighter weight concretes (EVA-C and EVA-FRC) were produced, which showed a drop of up to 34% in compressive strength when compared to concretes without replacement of stone aggregates (OC and FRC).
- In the three-point bending tests, it can be verified that the appearance of the first crack occurred at similar strength values for all the concretes investigated. After the formation of the first crack, the concrete with the replacement of coarse aggregate by EVA (EVA-C), the fiber-reinforced plain concrete (FRC), and the EVA fiber-reinforced concrete (EVA-FRC) maintained a residual strength of about 25%, 35%, and 52% respectively indicating that the hybridization of EVA with the addition of fibers improves the maintenance of post-peak strength in the investigated concretes. Besides, the toughness values for the FRC were approximately 20 J while the toughness for the EVA-FRC was approximately 30 J indicating that the addition of EVA is playing a role in bridging the crack opened.
- Applying the results obtained in the three-point bending tests for the FRC and the EVA-FRC in the design of industrial floors according to TR-34 showed that the EVA-FRC presented greater structural efficiency than the FRC for a cross-section of the same height (13 cm), considering the application of internal loads. Finally, the EVA particles play an important role in supporting the fiber to bridge the cracks, as could be seen by the constitutive analysis and by the three-point bending tests. Therefore, a pullout mechanism takes place in each EVA particle from the matrix before propagating the crack, improving the behavior of the fiber-reinforced 635 plain concrete.

ACKNOWLEDGEMENTS

This study was financed in part by the Coordenação de Aperfeiçoamento de Pessoal de Nível Superior (CAPES) – Brasil – Finance Code 001, by Brazilian funding agencies FAPERJ and 640 CNPq, and by Lafarge Holcim, with the donation of cement.

CITATIONS

- [1] F. K. Alqahtani and I. Zafar, "Plastic-based sustainable synthetic aggregate in Green Lightweight concrete: a review," *Constr. Build. Mater.*, vol. 292, pp. 123321, Jul 2021, <http://dx.doi.org/10.1016/j.conbuildmat.2021.123321>.
- [2] P. R. L. Lima, M. B. Leite, and E. Q. R. Santiago, "Recycled lightweight concrete made from footwear industry waste and CDW," *Waste Manag.*, vol. 30, no. 6, pp. 1107–1113, Jun 2010, <http://dx.doi.org/10.1016/j.wasman.2010.02.007>.
- [3] F. A. Salgado and F. A. Silva, "Recycled aggregates from construction and demolition waste towards an application on structural concrete: a review," *J. Build. Eng.*, vol. 52, pp. 104452, Jul 2022, <http://dx.doi.org/10.1016/j.jobe.2022.104452>.
- [4] H. P. Nguyen, A. Mueller, V. T. Nguyen, and C. T. Nguyen, "Development and characterization of lightweight aggregate recycled from construction and demolition waste mixed with other industrial by-products," *Constr. Build. Mater.*, vol. 313, pp. 125472, Dec 2021, <http://dx.doi.org/10.1016/j.conbuildmat.2021.125472>.
- [5] M. Contreras Llanes, M. Romero Pérez, M. J. Gázquez González, and J. P. Bolívar Raya, "Construction and demolition waste as recycled aggregate for environmentally friendly concrete paving," *Environ. Sci. Pollut. Res. Int.*, vol. 29, no. 7, pp. 9826–9840, Feb 2022, <http://dx.doi.org/10.1007/s11356-021-15849-4>.
- [6] J. A. Ferriz-Papi, E. Weekes, N. Whitehead, and A. Lee, "A cost-effective recycled aggregates classification procedure for construction and demolition waste evaluation," *Constr. Build. Mater.*, vol. 324, pp. 126642, Mar 2022, <http://dx.doi.org/10.1016/j.conbuildmat.2022.126642>.
- [7] F. G. Cunha, Z. L. M. Sampaio, and A. E. Martinelli, "Fiber-reinforced lightweight concrete formulated using multiple residues," *Constr. Build. Mater.*, vol. 308, pp. 125035, Nov 2021, <http://dx.doi.org/10.1016/j.conbuildmat.2021.125035>.
- [8] R. Ahmmad, M. Z. Jumaat, U. J. Alengaram, S. Bahri, M. A. Rehman, and H. Hashim, "Performance evaluation of palm oil clinker as coarse aggregate in high strength lightweight concrete," *J. Clean. Prod.*, vol. 112, pp. 566–574, Jan 2016, <http://dx.doi.org/10.1016/j.jclepro.2015.08.043>.

- [9] K. Piszcz-Karaś, M. Klein, J. Hupka, and J. Łuczak, "Utilization of shale cuttings in production of lightweight aggregates," *J. Environ. Manage.*, vol. 231, pp. 232–240, Feb 2019, <http://dx.doi.org/10.1016/j.jenvman.2018.09.101>.
- [10] N. Dulsang, P. Kasemsiri, P. Posi, S. Hiziroglu, and P. Chindaprasirt, "Characterization of an environment friendly lightweight concrete containing ethyl vinyl acetate waste," *Mater. Des.*, vol. 96, pp. 350–356, Apr 2016, <http://dx.doi.org/10.1016/j.matdes.2016.02.037>.
- [11] Z. L. M. Sampaio, A. E. Martinelli, and T. S. Gomes, "Formulation and characterization of structural lightweight concrete containing residues of porcelain tile polishing, tire rubber and limestone," *Ceramica*, vol. 63, no. 368, pp. 530–535, Oct 2017, <http://dx.doi.org/10.1590/0366-69132017633682139>.
- [12] X. Yang, J. Liu, H. Li, and Q. Ren, "Performance and ITZ of pervious concrete modified by vinyl acetate and ethylene copolymer dispersible powder," *Constr. Build. Mater.*, vol. 235, pp. 117532, Feb 2020, <http://dx.doi.org/10.1016/j.conbuildmat.2019.117532>.
- [13] A. Singh, P. V. Sampath, and K. P. Biligiri, "A review of sustainable pervious concrete systems: emphasis on clogging, material characterization, and environmental aspects," *Constr. Build. Mater.*, vol. 261, pp. 120491, Nov 2020, <http://dx.doi.org/10.1016/j.conbuildmat.2020.120491>.
- [14] S. Saoula, K. Ait Mokhtar, S. Haddadi, and E. Ghorbel, "Improvement of the performances of modified bituminous concrete with EVA and EVA-waste," *Phys. Procedia*, vol. 2, no. 3, pp. 1319–1326, Nov 2009, <http://dx.doi.org/10.1016/j.phpro.2009.11.098>.
- [15] S. Haddadi, E. Ghorbel, and N. Laradi, "Effects of the manufacturing process on the performances of the bituminous binders modified with EVA," *Constr. Build. Mater.*, vol. 22, no. 6, pp. 1212–1219, Jun 2008, <http://dx.doi.org/10.1016/j.conbuildmat.2007.01.028>.
- [16] A. Noor and M. A. U. Rehman, "A mini-review on the use of plastic waste as a modifier of the bituminous mix for flexible pavement," *Clean. Mater.*, vol. 4, pp. 100059, Jun 2022, <http://dx.doi.org/10.1016/j.clema.2022.100059>.
- [17] A. Chegenizadeh, L. Tokoni, H. Nikraz, and E. Dadras, "Effect of ethylene-vinyl acetate (EVA) on stone mastic asphalt (SMA) behaviour," *Constr. Build. Mater.*, vol. 272, pp. 121628, Feb 2021, <http://dx.doi.org/10.1016/j.conbuildmat.2020.121628>.
- [18] P. Panyakapo and M. Panyakapo, "Reuse of thermosetting plastic waste for lightweight concrete," *Waste Manag.*, vol. 28, no. 9, pp. 1581–1588, Jan 2008, <http://dx.doi.org/10.1016/j.wasman.2007.08.006>.
- [19] Z. Z. Ismail and E. A. AL-Hashmi, "Use of waste plastic in concrete mixture as aggregate replacement," *Waste Manag.*, vol. 28, no. 11, pp. 2041–2047, Nov 2008, <http://dx.doi.org/10.1016/j.wasman.2007.08.023>.
- [20] A. Kan and R. Demirboğa, "A novel material for lightweight concrete production," *Cement Concr. Compos.*, vol. 31, no. 7, pp. 489–495, Aug 2009, <http://dx.doi.org/10.1016/j.cemconcomp.2009.05.002>.
- [21] T. R. Naik, S. S. Singh, C. O. Huber, and B. S. Brodersen, "Use of post-consumer waste plastics in cement-based composites," *Cement Concr. Res.*, vol. 26, no. 10, pp. 1489–1492, Oct 1996, [http://dx.doi.org/10.1016/0008-8846\(96\)00135-4](http://dx.doi.org/10.1016/0008-8846(96)00135-4).
- [22] B. W. Jo, S. K. Park, and J. C. Park, "Mechanical properties of polymer concrete made with recycled PET and recycled concrete aggregates," *Constr. Build. Mater.*, vol. 22, no. 12, pp. 2281–2291, Dec 2008, <http://dx.doi.org/10.1016/j.conbuildmat.2007.10.009>.
- [23] S. C. Kou, G. Lee, C. S. Poon, and W. L. Lai, "Properties of lightweight aggregate concrete prepared with PVC granules derived from scraped PVC pipes," *Waste Manag.*, vol. 29, no. 2, pp. 621–628, Feb 2009, <http://dx.doi.org/10.1016/j.wasman.2008.06.014>.
- [24] F. K. Alqahtani, G. Ghataora, S. Dirar, M. I. Khan, and I. Zafar, "Experimental study to investigate the engineering and durability performance of concrete using synthetic aggregates," *Constr. Build. Mater.*, vol. 173, pp. 350–358, Jun 2018, <http://dx.doi.org/10.1016/j.conbuildmat.2018.04.018>.
- [25] F. K. Alqahtani, G. Ghataora, M. I. Khan, and S. Dirar, "Novel lightweight concrete containing manufactured plastic aggregate," *Constr. Build. Mater.*, vol. 148, pp. 386–397, Sep 2017, <http://dx.doi.org/10.1016/j.conbuildmat.2017.05.011>.
- [26] Y. W. Choi, D. J. Moon, J. S. Chung, and S. K. Cho, "Effects of waste PET bottles aggregate on the properties of concrete," *Cement Concr. Res.*, vol. 35, no. 4, pp. 776–781, Apr 2005, <http://dx.doi.org/10.1016/j.cemconres.2004.05.014>.
- [27] D. C. Jansen et al., "Lightweight fly ash-plastic aggregates in concrete," *Transp. Res. Rec.*, vol. 1775, no. 1, pp. 44–52, Jan 2001, <http://dx.doi.org/10.3141/1775-07>.
- [28] H. Li et al., "Improvements in setting behavior and strengths of cement paste/mortar with EVA redispersible powder using C-S-Hs-PCE," *Constr. Build. Mater.*, vol. 262, pp. 120097, Nov 2020, <http://dx.doi.org/10.1016/j.conbuildmat.2020.120097>.
- [29] Y. W. Choi, D. J. Moon, Y. J. Kim, and M. Lachemi, "Characteristics of mortar and concrete containing fine aggregate manufactured from recycled waste polyethylene terephthalate bottles," *Constr. Build. Mater.*, vol. 23, no. 8, pp. 2829–2835, Aug 2009, <http://dx.doi.org/10.1016/j.conbuildmat.2009.02.036>.
- [30] G. Sang, Y. Zhu, and G. Yang, "Mechanical properties of high porosity cement-based foam materials modified by EVA," *Constr. Build. Mater.*, vol. 112, pp. 648–653, Jun 2016, <http://dx.doi.org/10.1016/j.conbuildmat.2016.02.145>.
- [31] K. A. Khan, I. Ahmad, and M. Alam, "Effect of Ethylene Vinyl Acetate (EVA) on the setting time of cement at different temperatures as well as on the mechanical strength of concrete," *Arab. J. Sci. Eng.*, vol. 44, no. 5, pp. 4075–4084, 2019, <http://dx.doi.org/10.1007/s13369-018-3249-4>.

- [32] C. Brovelli, L. Hilliou, Y. Hemar, J. Pais, P. Pereira, and M. Crispino, "Rheological characteristics of EVA modified bitumen and their correlations with bitumen concrete properties," *Constr. Build. Mater.*, vol. 48, pp. 1202–1208, Nov 2013, <http://dx.doi.org/10.1016/j.conbuildmat.2013.07.032>.
- [33] A. Ben Fraj, M. Kismi, and P. Mounanga, "Valorization of coarse rigid polyurethane foam waste in lightweight aggregate concrete," *Constr. Build. Mater.*, vol. 24, no. 6, pp. 1069–1077, Jun 2010, <http://dx.doi.org/10.1016/j.conbuildmat.2009.11.010>.
- [34] E. Rahmani, M. Dehestani, M. H. A. Beygi, H. Allahyari, and I. M. Nikbin, "On the mechanical properties of concrete containing waste PET particles," *Constr. Build. Mater.*, vol. 47, pp. 1302–1308, Oct 2013, <http://dx.doi.org/10.1016/j.conbuildmat.2013.06.041>.
- [35] M. Batayneh, I. Marie, and I. Asi, "Use of selected waste materials in concrete mixes," *Waste Manag.*, vol. 27, no. 12, pp. 1870–1876, Jan 2007, <http://dx.doi.org/10.1016/j.wasman.2006.07.026>.
- [36] W. C. Tang, Y. Lo, and A. Nadeem, "Mechanical and drying shrinkage properties of structural-graded polystyrene aggregate concrete," *Cement Concr. Compos.*, vol. 30, no. 5, pp. 403–409, May 2008, <http://dx.doi.org/10.1016/j.cemconcomp.2008.01.002>.
- [37] B. Chen and J. Liu, "Properties of lightweight expanded polystyrene concrete reinforced with steel fiber," *Cement Concr. Res.*, vol. 34, no. 7, pp. 1259–1263, Jul 2004, <http://dx.doi.org/10.1016/j.cemconres.2003.12.014>.
- [38] A. Bentur and S. Mindess, *Fibre Reinforced Cementitious Composites*. London: Taylor & Francis, 2007.
- [39] R. Jain, R. Gupta, M. Khare, and D. Ashish, "Use of polypropylene fiber reinforced concrete as a construction material for rigid pavements," *Indian Concr. J.*, vol. 85, pp. 45–53, Mar 2011.
- [40] J. Roesler, S. Altoubat, D. Lange, K.-A. Rieder, and G. Ulreich, "Effect of synthetic fibers on structural behavior of concrete slabs on ground," *ACI Mater. J.*, vol. 103, pp. 3, Jan 2006.
- [41] V. N. Lima, D. C. T. Cardoso, and F. A. Silva, "Creep mechanisms in precracked polypropylene and steel fiber-reinforced concrete," *J. Mater. Civ. Eng.*, vol. 33, no. 8, pp. 04021187, May 2021, [http://dx.doi.org/10.1061/\(ASCE\)MT.1943-5533.0003775](http://dx.doi.org/10.1061/(ASCE)MT.1943-5533.0003775).
- [42] D. T. C. Madhavi, L. S. Raju, and D. Mathur, "Polypropylene fiber reinforced concrete," *RE-view*, 2014.
- [43] O. Ozturk and N. Ozyurt, "Sustainability and cost-effectiveness of steel and polypropylene fiber reinforced concrete pavement mixtures," *J. Clean. Prod.*, vol. 363, pp. 132582, Aug 2022, <http://dx.doi.org/10.1016/j.jclepro.2022.132582>.
- [44] F. R. Souza, "Concreto reforçado com fibras de PVA aplicado a pavimentos aeroportuários: propriedades mecânicas e dimensionamento," Ph.D. dissertation, Pontif. Univ. Catol. Rio de Janeiro, Rio de Janeiro, 2021.
- [45] R. P. Manfredi, "Dimensionamento de compósitos cimentícios reforçados com fibras de aço," M.S. thesis, Pontif. Univ. Catol. Rio de Janeiro, Rio de Janeiro, 2020.
- [46] B. Ali, L. A. Qureshi, and R. Kurda, "Environmental and economic benefits of steel, glass, and polypropylene fiber reinforced cement composite application in jointed plain concrete pavement," *Compos. Commun.*, vol. 22, pp. 100437, 2020, <http://dx.doi.org/10.1016/j.coco.2020.100437>.
- [47] C. Y. Sung and K. S. Nam, "Flexural performance of polypropylene fiber reinforced EVA concrete," *J. Korean Soc. Agric. Eng.*, vol. 58, no. 2, pp. 83–90, Mar 2016, <http://dx.doi.org/10.5389/KSAE.2016.58.2.083>.
- [48] K. S. Nam and C. Y. Sung, "The compressive strength and durability properties of polypropylene fiber reinforced EVA concrete," *J. Korean Soc. Agric. Eng.*, vol. 57, no. 4, pp. 11–19, Jul 2015, <http://dx.doi.org/10.5389/KSAE.2015.57.4.011>.
- [49] J. F. Natalli, E. C. S. Thomaz, J. C. Mendes, and R. A. F. Peixoto, "A review on the evolution of Portland cement and chemical admixtures in Brazil," *Rev. IBRACON Estrut. Mater.*, vol. 14, no. 6, pp. 14603, 2021, <http://dx.doi.org/10.1590/s1983-41952021000600003>.
- [50] Associação Brasileira de Normas Técnicas, *Cimento Portland – Requisitos*, ABNT NBR 16697, 2018.
- [51] Associação Brasileira de Normas Técnicas, *Agregados para Concreto*, ABNT NBR 7211, 2005.
- [52] Associação Brasileira de Normas Técnicas, *Aditivos para Concreto de Cimento Portland*, ABNT NBR 11768, 1992.
- [53] Associação Brasileira de Normas Técnicas, *Concreto – Determinação da Consistência pelo Abatimento do Tronco de Cone*, ABNT NBR NM 67, 1998.
- [54] Associação Brasileira de Normas Técnicas, *Concreto – Ensaio de Compressão de Corpos de Prova Cilíndricos*, ABNT NBR 5739, 2007.
- [55] Associação Brasileira de Normas Técnicas, *Concreto – Determinação do Módulo Elástico de Elasticidade à Compressão*, ABNT NBR 8522, 2008.
- [56] European Standard, *Test Method for Metallic Fibered Concrete – Measuring the Flexural Tensile Strength (Limit of Proportionality (LOP), Residual)*, EN 14651, 2005.
- [57] fib, *fib Model Code*. Switzerland, 2010.
- [58] American Society for Testing and Materials, *Standard Test Method for Length Change of Hardened Hydraulic-Cement Mortar and Concrete*, ASTM C157, 2017.
- [59] American Society for Testing and Materials, *Standard Practice for Use of Apparatus for the Determination of Length Change of Hardened Cement Paste, Mortar, and Concrete BT - Standard Practice for Use of Apparatus for the Determination of Length Change of Hardened Cement Paste, Mortar, and Concrete*, ASTM C490, 2017.

- [60] The Concrete Society, *Concrete Industrial Ground Floor Slabs: a Guide to Their Design and Construction* (Technical Report 34). Berkshire, 2013.
- [61] L. R. Brancher, M. Nunes, A. Grisa, D. Pagnussat, and M. Zeni, "Acoustic behavior of subfloor lightweight mortars containing micronized poly (Ethylene Vinyl Acetate) (EVA)," *Materials*, vol. 9, no. 1, pp. 51, Jan 2016, <http://dx.doi.org/10.3390/ma9010051>.
- [62] W. Shen, R. Dong, J. Li, M. Zhou, W. Ma, and J. Zha, "Experimental investigation on aggregate interlocking concrete prepared with scattering-filling coarse aggregate process," *Constr. Build. Mater.*, vol. 24, no. 11, pp. 2312–2316, Nov 2010, <http://dx.doi.org/10.1016/j.conbuildmat.2010.04.023>.
- [63] M. Pundir, M. Tirassa, M. Fernández Ruiz, A. Muttoni, and G. Anciaux, "Review of fundamental assumptions of the Two-Phase model for aggregate interlocking in cracked concrete using numerical methods and experimental evidence," *Cement Concr. Res.*, vol. 125, pp. 105855, Nov 2019, <http://dx.doi.org/10.1016/j.cemconres.2019.105855>.
- [64] Y. Yang, B. Yuan, Q. Sun, X. Tang, and X. Yingquan, "Mechanical properties of EVA-modified cement for underground gas storage," *J. Nat. Gas Sci. Eng.*, vol. 27, pp. 1846–1851, Nov 2015, <http://dx.doi.org/10.1016/j.jngse.2015.11.013>.
- [65] H. Li et al., "Influence of defoaming agents on mechanical performances and pore characteristics of Portland cement paste/mortar in presence of EVA dispersible powder," *J. Build. Eng.*, vol. 41, pp. 102780, Sep 2021, <http://dx.doi.org/10.1016/j.jobe.2021.102780>.
- [66] V. N. Lima, "Fluência e propriedades mecânicas de compósitos cimentícios reforçados com fibra de aço e polipropileno," Ph.D. dissertation, Pontif. Univ. Catol. Rio de Janeiro, Rio de Janeiro, 2019.
- [67] P. D. Nieuwoudt, "Time-dependent behaviour of cracked steel fibre reinforced concrete: from single fibre level to macroscopic level," M.S. thesis, Stellenbosch Univ., Stellenbosch, 2016.
- [68] J. Brito and N. Saikia, "Recycled aggregate in concrete: use of industrial, construction and demolition waste," *Green Energy Technol.*, vol. 54, 2013, <http://dx.doi.org/10.1007/978-1-4471-4540-0>.
- [69] S. Yin, R. Tuladhar, T. Collister, M. Combe, N. Sivakugan, and Z. Deng, "Post-cracking performance of recycled polypropylene fibre in concrete," *Constr. Build. Mater.*, vol. 101, pp. 1069–1077, Dec 2015, <http://dx.doi.org/10.1016/j.conbuildmat.2015.10.056>.
- [70] R. S. Castoldi, L. M. S. Souza, and F. A. Silva, "Comparative study on the mechanical behavior and durability of polypropylene and sisal fiber reinforced concretes," *Constr. Build. Mater.*, vol. 211, pp. 617–628, Jun 2019, <http://dx.doi.org/10.1016/j.conbuildmat.2019.03.282>.
- [71] V. N. Lima, D. C. T. Cardoso, and F. A. Silva, "Flexural creep behavior of steel and polypropylene fiber reinforced concrete," in *Proc. 10th Int. Conf. Fract. Mech. Concr. Concr. Struct.*, 2019, <http://dx.doi.org/10.21012/FC10.234778>.
- [72] R. P. Manfredi, F. A. Silva, and D. C. T. Cardoso, "On punching shear strength of steel fiber-reinforced concrete slabs-on-ground," *ACI Struct. J.*, vol. 119, no. 4, pp. 185–196, Jul 2022, <http://dx.doi.org/10.14359/51734520>.
- [73] T. Fujiwara, "Effect of aggregate on drying shrinkage of concrete," *J. Adv. Concr. Technol.*, vol. 6, no. 1, pp. 31–44, Feb 2008, <http://dx.doi.org/10.3151/jact.6.31>.
- [74] A. K. H. Kwan, W. W. S. Fung, and H. H. C. Wong, "Reducing drying shrinkage of concrete by treatment of aggregate," *Mag. Concr. Res.*, vol. 62, no. 6, pp. 435–442, May 2010, <http://dx.doi.org/10.1680/mac.2010.62.6.435>.
- [75] S. Ismail and M. Ramli, "Mechanical strength and drying shrinkage properties of concrete containing treated coarse recycled concrete aggregates," *Constr. Build. Mater.*, vol. 68, pp. 726–739, Oct 2014, <http://dx.doi.org/10.1016/j.conbuildmat.2014.06.058>.
- [76] M. E. Karaguler and M. S. Yatagan, "Effect of aggregate size on the restrained shrinkage of the concrete and mortar," *MOJ Civ. Eng.*, vol. 4, no. 1, pp. 15–21, Jan 2018, <http://dx.doi.org/10.15406/mojce.2018.04.00092>.

Author contributions: INL, FRS, FPT: data curation, methodology, formal analysis; VNL: conceptualization, data curation, formal analysis, methodology, writing original draft; MIBR, FAS: conceptualization, funding acquisition, supervision.

Editors: Diogo Ribeiro, Guilherme Aris Parsekian.